Title	Measurements of neutron total and capture cross sections of ^{241}Am with ANNRI at J-PARC
Author(s)	Terada Kazushi, Kimura Atsushi, Nakao Taro, Nakamura Shoji, Mizuyama Kazuhito, Iwamoto Nobuyuki, Iwamoto Osamu, Harada Hideo, Katabuchi Tatsuya, Igashira Masayuki, Sano Tadafumi, Takahashi Yoshiyuki, Pyeon C. H., Fukutani Satoshi, Fujii Toshiyuki, Yagi Takahiro, Takamiya Koichi, Hori Junichi
Citation	Journal of Nuclear Science and Technology,55(10),p.1198-1211
Text Version	Accepted Manuscript
URL	https://jopss.jaea.go.jp/search/servlet/search?5061362
DOI	https://doi.org/10.1080/00223131.2018.1485519
Right	This is an Accepted Manuscript of an article published by Taylor & Francis in Journal of Nuclear Science and Technology on October 2018, available at http://www.tandfonline.com/10.1080/00223131.2018.1485519.

ARTICLE

Typeset with jnst.cls <ver.2.1>

Measurements of neutron total and capture cross sections of ^{241}Am with ANNRI at J-PARC

Kazushi Terada[1]*, Atsushi Kimura[1]†, Taro Nakao[1], Shoji Nakamura[1], Kazuhito Mizuyama[1], Nobuyuki Iwamoto[1], Osamu Iwamoto[1], Hideo Harada[1],Tatsuya Katabuchi[2], Masayuki Igashira[2], Tadafumi Sano[3], Yoshiyuki Takahashi[3], Cheol Ho Pyeon[3], Satoshi Fukutani[3], Toshiyuki Fujii[3]‡, Takahiro Yagi[3], Koichi Takamiya[3] and Jun-ichi Hori[3]

[1]*Japan Atomic Energy Agency, 2-4 Shirakata, Tokai-mura, Naka-gun, Ibaraki 311-1195, Japan;*

[2]*Tokyo Institute of Technology, 2-12-1-N1-26 Ookayama, Meguro-ku, Tokyo 152-8550, Japan;*

[3]*Kyoto University Research Reactor Institute, Kumatori-cho, Sennan-gun, Osaka 590-0494, Japan.*

Neutron total and capture cross sections of ^{241}Am have been measured with a new data acquisition system and a new neutron transmission measurement system installed in Accurate Neutron Nucleus Reaction measurement Instrument (ANNRI) at Materials and Life Science Experimental Facility (MLF) of Japan Proton Accelerator Research Complex (J-PARC). The neutron total cross sections of ^{241}Am were determined by using a neutron time-of-flight method in the neutron energy region from 4 meV to 2 eV. The thermal total cross section of ^{241}Am was derived with an uncertainty of 2.9%. A pulse-height weighting technique was applied to determine neutron capture yields of ^{241}Am. The neutron capture cross sections were determined by the time-of-flight method in the neutron energy region from the thermal to 100 eV, and the thermal capture cross section was obtained with an uncertainty of 4.0%. The evaluation data of JENDL-4.0 and JEFF-3.2 were compared with the present results.

Keywords: neutron total cross section, neutron capture cross section, americium 241, ANNRI, PHITS

1. Introduction

Accurate nuclear data are indispensable for the study of nuclear transmutation system. Sensitivity and uncertainty analyses of reactor physics parameters were performed recently for the accelerator-driven system (ADS) proposed by the Japan Atomic Energy Agency (JAEA) using the covariance of JENDL-4.0[1, 2]. Impact of improving accuracy of relevant nuclear data was quantitatively shown, for example, the uncertainty of k_{eff} was estimated to be about 1% that is about 3 times larger than the required accuracy for designing the reactor system. According to the investigation, capture cross sections of minor actinides (MAs) are one of the most important data[3]. Especially, the uncertainty of capture cross section on ^{241}Am has large contributions in the uncertainties of neutronics characteristics in the ADS core. However, the current accuracy is so large as 7% for the capture cross section[2, 3] . In consideration of this situation, the improvement of the accuracy of this cross section will have a great impact for the study of ADS systems.

To meet the requirement, a research project entitled "Research and development for Accuracy Improvement of neutron nuclear data on Minor ACtinides (AIMAC)" was started[4, 5]. The challenging goal of the project was to reduce the uncertainties of the capture cross sections of ^{237}Np and ^{241,243}Am to half of the present values by integrating specialists' leading-edge knowledge and techniques. As one of the approaches for confirming the accuracy of the measurements, to reduce systematic uncertainties, a consistency check of two independent measurements was considered to be effective. In the case of the neutron cross sections of ^{241}Am, its capture neutron cross section accounts for 98-99% of its total neutron cross section at low energy region. Therefore, the comparison between total and capture cross sections can be used for this consistency check in the case of ^{241}Am. To enable this comparison, a new data acquisition (DAQ) system and a new neutron transmission measurement system have been developed

*Present address: Tokyo Institute of Technology, 4259-B67 Nagatsuda, Midori-ku, Yokohama 226-8501, Japan.
†Corresponding author. Email: kimura.atsushi04@jaea.go.jp
‡Present address: Osaka University, 2-1 Yamadaoka, Suita, Osaka 565-0871, Japan.

in ANNRI at MLF in J-PARC[6]. The new DAQ system achieved 90% live time for 100 kcps event rate. Moreover, we have developed the techniques accurately determining the sample mass by two different methods: calorimetric method, and gamma-ray spectroscopic method[7]. The reason is that uncertainty due to the sample mass is one of the most important factors contributing to the discrepancies of measured cross section data[9–12]. These approaches enable us to reduce the uncertainty on both neutron total and capture cross section measurements.

In the past, several measurements of neutron total cross sections of ^{241}Am have been performed[13–19]. **Figure 1** shows the present status on total cross sections of ^{241}Am. A large discrepancy exists among the previous measurements at the first and second resonances. It was also pointed that there is an inconsistency between measured neutron total and capture cross sections of ^{241}Am. Precise measurements of neutron total cross sections for ^{241}Am are indispensable. In addition, various measurements of neutron capture cross sections on ^{241}Am have been carried out by activation and time-of-flight (TOF) methods[10, 17, 20–35]. Currently, there are discrepancies among the previous measurements of the thermal neutron capture cross section of ^{241}Am[36]. These discrepancies cause the large uncertainty of the current evaluated nuclear data.

[Figure 1 about here.]

From the viewpoint described above, we measured the neutron total and capture cross sections of ^{241}Am by utilizing the state-of-art techniques. The measurements of neutron total cross sections of ^{241}Am are described in Section 2. The measurements of neutron capture cross sections of ^{241}Am are mentioned in Section 3. Finally, the conclusion is given in Section 4.

2. Neutron total cross section measurements

2.1. Experimental procedure

Neutron total cross sections of ^{241}Am were measured with ANNRI at the MLF of the J-PARC. An ^{241}Am sample having an activity of 957 MBq and a dummy sample were prepared for

measurements of neutron total and capture cross sections. Neutron transmission TOF spectra for the samples have been measured with two types of Li-glass scintillation detectors. The details of experimental procedure and data analysis were described in Ref.[6], so it is briefly described in below.

J-PARC accelerator

Neutrons were produced via the spallation reactions induced by a 3-GeV proton beam impinging on a mercury target of the MLF[37]. The 3 GeV rapid cycling synchrotron was operated in single bunch mode with a repetition rate of 25 Hz. The proton beam power on the spallation target was 195 kW in the total cross section measurements. The neutrons emitted from the spallation target were moderated by liquid hydrogen moderators cooled at 19 K and were guided into the ANNRI. A signal from a proton beam pulse monitor located in a beam transport tube to the spallation target was used as the start trigger for the TOF measurements. The number of proton beam pulses was recorded and used for normalization of each measurement.

Samples

The characteristics of the ^{241}Am and the dummy samples are summarized in **Table 1**. The Am sample was prepared by compression molding of mixtures of AmO_2 powder and Y_2O_3 powder into the form of a pellet with a diameter of 10.0 ± 0.1 mm and a thickness of 0.5 ± 0.1 mm, then the pellet was sealed in Al containers with a thickness of 0.1 mm. Similarly, the dummy sample, which contains a Y_2O_3 pellet, was prepared. For the derivation of the number of ^{241}Am atoms, the activity of the Am sample was determined with a calorimetric method. Decay heat of the Am sample was measured accurately with a precision of 200 nW by using the TAM-IV calorimeter manufactured by TA Instruments, and thus the activity of the Am sample was obtained with an uncertainty of 0.45%[7]. The isotopic composition of the Am sample was analyzed by thermal ionization mass spectrometry and alpha-ray spectroscopy[8]. The determined

isotopic purity of ^{241}Am was 99.9% , and the isotopic contamination of ^{239}Pu was 0.09%.

[Table 1 about here.]

Transmission measurements

These samples were placed at the most upper stream part of the intermediate collimator having a diameter of 9 mm installed in the ANNRI[38, 39]. The distance between the moderator and the samples was 24 m. Two types of Li-glass scintillation detectors were utilized for transmission measurements. A GS20 ^{6}Li-glass detector (PMT:H7195) manufactured by OKEN with dimensions of 50 mm x 50 mm and a thickness of 1 mm using enriched ^{6}Li (^{6}Li > 95%) was used to obtain transmission neutron TOF spectra. Neutrons passing through the samples are detected by the ^{6}Li-glass detector via the ^{6}Li(n,α)^{3}H reactions. Additionally, to determine background except for neutrons, a GS30 ^{7}Li-glass detector (^{7}Li > 99.99%) with same size of the ^{6}Li-glass detector was used. The ^{7}Li-glass detector was located on the upstream side of the ^{6}Li-glass detector. Distance from the moderator to the ^{6}Li-glass detector was 27.8 m. Signals from these detectors were fed into the DAQ with a CAEN V1720 (12bit 250MHz) module to calculate timing and pulse height (PH) data. The timing and pulse height data were recorded in an event-by-event mode. Measurements were carried out with a lead block having a thickness of 5.0 cm placed on the neutron beam line in order to reduce the dead time of the Li-glass detectors caused by intense gamma-rays from the moderator. The black resonance technique was applied using neutron notch filters of ^{nat}Mn, ^{nat}Co, ^{nat}In and ^{nat}Ag to estimate the background due to frame-overlap neutrons. The measuring times of the ^{241}Am and the dummy samples were 8 h and 7 h, respectively.

2.2. Data analysis

Figure 2 shows PH spectra of the ^{241}Am sample measured with the ^{6}Li-glass detector and the ^{7}Li-glass detector. Peaks around 3500 ch. are due to the ^{6}Li(n,α)^{3}H reactions. Double-hit

and triple-hit peaks were also observed in the spectrum measured by the ^{6}Li-glass detector. The double-hit and triple-hit peaks were enough small comparison to the single-hit peak, and the influence of the double-hit and triple-hit events were negligible in this measurement. The background caused by gamma-rays existing on the beam line was obtained by the ^{7}Li-glass detector. Incidentally, the ^{7}Li-glass detector contains slight amount of ^{6}Li (0.01%), the ^{6}Li(n,α)^{3}H peak was also observed by the ^{7}Li-glass detector. One gate was set in these spectra from 2450 ch. to 4650 ch., as shown in **Figure 2**, and gated TOF spectra were derived.

[Figure 2 about here.]

Figure 3 indicates the gated TOF spectra of the ^{241}Am and the dummy samples measured with the ^{6}Li-glass detector and the ^{7}Li-glass detector. Two small dips from 7×10^{5} ch. to 1×10^{6} ch. observed in the ^{6}Li-glass spectrum of the ^{241}Am sample are attributed to resonance absorption by the ^{241}Am sample. Large dips at 2.4×10^{5} ch. and 4.3×10^{5} ch. were caused by the neutron filters (^{nat}Ag and ^{nat}In). The broad peak around 7×10^{6} ch is the thermalized neutron bump made by the liquid hydrogen moderator. The gamma-ray backgrounds were smaller than the neutron TOF spectra by two orders of magnitude.

[Figure 3 about here.]

Dead time corrections were made for the gated neutron TOF using a fixed dead time of 1264 ns due to the settings of the CAEN V1720. The dead time corrections were 1.2% and 8.0% at the ^{241}Am first resonance (0.31 eV) and the thermal neutron energy, respectively. The dead time for the ^{7}Li-glass detector was negligibly small in this experiment.

The net neutron TOF spectra of the ^{241}Am and the dummy samples were determined by subtracting the backgrounds caused by gamma-rays and frame-overlap neutrons. The gamma-ray backgrounds were deduced from the gated neutron TOF spectra with the ^{7}Li-glass detector. For the estimation of the frame-overlap neutron background, the gated neutron TOF spectra from 37 ms to 40 ms were fitted by an exponential decay function, and the fitted function was shifted to the left side by 40 ms. **Figure 4** indicates the determined frame overlap background of

the ^{241}Am sample. The deduced back ground shows good agreement with the black resonance of ^{145}In (1.46 eV).

[Figure 4 about here.]

Finally, neutron total cross sections of ^{241}Am, σ_{total}, were determined as follows:

$$\exp(-n\sigma_{\text{total}}) = T = \frac{C_{\text{Am}} - B^{\gamma}_{\text{Am}} - B^{FO}_{\text{Am}}}{C_{\text{Dummy}} - B^{\gamma}_{\text{Dummy}} - B^{FO}_{\text{Dummy}}} \tag{1}$$

where n is the areal density of the ^{241}Am sample (atoms/b), T is the neutron transmission ratio of the ^{241}Am sample, C is the gated neutron TOF spectrum normalized with incident neutron intensity for each sample, B^{γ} is the background due to gamma-rays and B^{FO} is the background caused by the frame overlap neutrons. Neutron beam intensity determined by the number of the incident protons was used in order to normalize the neutron transmission ratio of ^{241}Am. **Figure 5** shows the obtained neutron transmission ratio of ^{241}Am. The thickness of the ^{241}Am sample was determined to be $2.40 \pm 0.05 \times 10^{-5}$ atoms/b. This uncertainty was mainly caused by the uncertainty of ^{241}Am sample diameter (10.0 ± 0.1 mm). Correction for incident neutron intensity was 0.47% by considering the number of the incident protons. The main component of the uncertainty for the neutron total cross section comes from the uncertainty of the sample diameter.

[Figure 5 about here.]

2.3. Results and discussion

The derived total cross section of ^{241}Am is shown in **Fig. 6**. The previous measurement of Adamchuk *et al.*[13], evaluated cross sections of JENDL-4.0[40] and JEFF-3.2[41] are also illustrated. The obtained total cross section at thermal energy was derived as 730 ± 21 b. Adamchuk *et al.*[13] measured the total cross sections of ^{241}Am in the neutron energy region from 6.3 meV to 82 eV using a reactor at Dubna. They prepared two ^{241}Am samples with thicknesses of 0.521 and 0.0665 g/cm. Two types of BF_3 detectors were used for neutron transmission mea-

surements. Their results are systematically smaller than the present results by 15%. It might be caused by the incorrect sample thicknesses or a normalization of incident neutrons. In comparison with the present results, the evaluated thermal total cross section of JENDL-4.0 is 4.2% smaller, and that of JEFF-3.2 is 4.7% larger. ENDF/B-VII.1[42] has adopted the same value as JENDL-4.0.

[Figure 6 about here.]

3. Neutron capture cross section measurements

3.1. Experimental procedure

Measurements of neutron capture cross sections of ^{241}Am have been performed at the ANNRI of the MLF. The ^{241}Am sample was placed at the sample position of the array of Ge detectors having a flight length of 21.5 m from the moderator and gamma-rays emitted from the sample were measured. The array of Ge detectors is composed of two cluster-Ge detectors, eight coaxial-Ge detectors and anti-coincidence shields around each Ge detector[43]. In the measurements, two cluster Ge detectors were used, but the coaxial Ge detectors were not used because they suffered from severe electrical noise. Additionally, a lead plate with a thickness of 5 mm was placed in front of each cluster Ge detector for attenuation of the intense decay gamma-rays from ^{241}Am. The signals from the cluster-Ge detectors were digitized and analyzed with CAEN V1724 (14 bit, 100 MHz) ADC boards[6]. The TOF and PH data were recorded in list-mode. The peak efficiency was 2.28 ± 0.11% at 1332 keV gamma-rays[44].

The accelerator was operated in a single bunch mode at a repetition rate of 25 Hz. The proton beam power was 205 kW. The neutron beam was collimated to a diameter of 22 mm at the sample position. Neutrons traveled through a neutron beam duct, which housed the sample. Helium gas ran through the beam duct to reduce scattering neutron background by air.

The same ^{241}Am and the dummy samples were used as described in Chap. 2.1. A ^{197}Au sample with a diameter of 10.0 ± 0.1 mm and a weight of 174 ± 1 mg was used as a standard for PH

weighting technique (PHWT)[45]. An enriched ^{10}B sample with a diameter of 10.0 ± 0.2 mm was utilized to determine the shape of the incident neutron energy spectrum. To estimate background due to scattered neutrons by the ^{241}Am sample, an enriched ^{208}Pb sample with a diameter of 5.0 ± 0.1 mm and a weight of 170 ± 1 mg was also used. All samples were packaged in bags made of fluorinated ethylene- propylene copolymer (FEP) films. Measurement of the FEP bag without any sample (Blank) was carried out for background estimation in case of the "no sample condition". The measuring times were summarized in **Table 2**.

[Table 2 about here.]

3.2. Data analysis

Incident neutron energy spectrum

The incident neutron energy spectrum was determined by measuring 478 keV gamma-rays from ^{10}B(n, $\alpha\gamma$)^{7}Li reactions. TOF spectra gated in the 478 keV peak region were made for the ^{10}B, ^{208}Pb and blank measurements. Sample-independent and sample-scattered neutron backgrounds were estimated using the TOF spectra of blank and ^{208}Pb measurements and subtracted from the ^{10}B TOF spectrum. The cross section data of the ^{10}B(n, $\alpha\gamma$)^{7}Li reaction in JENDL-4.0[46] were used to convert the detected counts to the number of the incident neutrons. The dead time correction was made for the each TOF spectrum. The correction of the neutron self-shielding and multiple scattering in the ^{10}B sample was made by using the Monte-Carlo simulation code PHITS[47]. The cross section data used for the calculation were taken from JENDL-4.0. **Figure 7** shows the derived correction factor. In this calculation, the uncertainty of the corrections were deduced from the uncertainties of the ^{10}B sample diameter and mass. The value was 2.3% for thermal energy neutrons. The obtained incident neutron energy spectrum is shown in **Fig. 8**. The broad peak around 10 meV corresponds to the neutron bump thermalized in the liquid hydrogen moderator. The spectrum shows the typical $1/E$ energy dependence from 0.1 to 100 eV.

[Figure 7 about here.]

[Figure 8 about here.]

PH weighting technique

A PHWT[45] was applied to derive neutron capture yields of the ^{241}Am and ^{197}Au samples. PHWT is based on the physical fact that the total energy sum of the emitted gamma-rays following each capture reaction is equal to $B_n + E_n$, where B_n is the neutron binding energy of the target nucleus and E_n is the center-of-mass energy of the incident neutron. In PHWT, the neutron capture yield Y is calculated as follows:

$$Y = \frac{\sum_I W(I)S(I)}{B_\mathrm{n} + E_\mathrm{n}}, \tag{2}$$

where $W(I)$ is the weighting function of each cluster Ge detector, I is the channel number, $S(I)$ is a PH spectrum. The weighting function $W(I)$ was built from detector response functions. In this paper, weighting function $W(I)$ was normalized using the neutron capture cross section of ^{197}Au in JENDL-4.0[49] at thermal energy. The neutron capture cross sections of ^{241}Am, $\sigma_\mathrm{Am}(E_n)$, depending on incident neutron energy were obtained from the following equation:

$$\sigma_\mathrm{Am}(E_n) = Y \cdot \frac{P_\mathrm{Au}}{P_\mathrm{Am}} \cdot \frac{\phi(E_{th})}{\phi(E_n)} \cdot \frac{1}{n_\mathrm{Am}}, \tag{3}$$

where P is the number of incident protons for each sample, $\phi(E_n)$ is the number of incident neutrons, E_n is neutron energy, E_{th} is thermal neutron energy, and n_Am is the number of the ^{241}Am atoms. The number of the ^{241}Am atoms was derived by using the calorimeter, as described before.

For the present experimental setup, the response functions of the cluster-Ge detectors were calculated by Monte Carlo simulation using the Geant4 code[48]. A comparison between calculated and measured response functions for a ^{60}Co source is shown in **Fig. 9**. The peak areas on the 1173 and 1332 keV obtained by the Geant4 simulations were larger than the measured

values by 0.6% and 1.9%, respectively. The cause of difference is that the measured 1173 and 1332 keV peaks have a contribution of low energy tails. Below 200 keV, the measured spectra is smaller than the simulated result due to the threshold on the signal processing. Below a gamma-ray energy of 1000 keV, we calculated the response functions every 100 keV. In the gamma-ray energy region from 1000 keV to 10000 keV, the response functions were calculated every 1000 keV.

[Figure 9 about here.]

The weighting function was calculated from the corresponding response functions by assuming a trial function. Finally, the weighting function was normalized using the measurements of the Au sample and evaluated capture cross section of ^{197}Au in JENDL-4.0 in the neutron range from 24.3 to 26.3 meV. **Figure 10** indicates the calculated weighting function for the ^{241}Am sample as an example. The deduced weighting function $W(I)$ is described as follows:

$$W(I) = \sum_{n=1}^{4} a_n I^n \tag{4}$$

$$\begin{aligned} a_1 &= 3.4929 \times 10^{-1} \\ a_2 &= -6.4250 \times 10^{-5} \\ a_3 &= 1.6766 \times 10^{-9} \\ a_4 &= -1.3572 \times 10^{-12}, \end{aligned} \tag{5}$$

[Figure 10 about here.]

The uncertainty of the weighting function was evaluated using the following equation:

$$RSS = \frac{\left\{\sum_I W(I) R\left(I, E_\gamma\right) - k \cdot E_\gamma\right\}^2}{(L-N) \cdot E_\gamma^2} \tag{6}$$

where $R\left(I, E_\gamma\right)$ is the calculated response functions, E_γ is gamma-ray energy, k is the normalization factor of the weighting function. L is the number of response functions and N is the number of degrees of freedom for the weighting function. The uncertainties of weighting func-

tions caused by the response functions were estimated as 1%.

Figure 11 shows PH spectra for the ^{241}Am, dummy, blank and ^{208}Pb measurements. These PH spectra except for the blank measurement were obtained by subtracting sample-independent background estimated from the PH spectra for the blank measurement. The PH spectrum for the ^{241}Am decay measurement is also shown in the figure. The number of proton beam pulses was used for normalization in background subtraction. A difference appeared clearly between the ^{241}Am and dummy PH spectra below the Q-value of ^{241}Am(n, γ) reaction (5538 keV). Additionally, backgrounds due to neutron capture reactions by the materials other than AmO_2 (aluminum case and Y_2O_3) were also observed. For example, a 7724 keV prompt gamma-ray peak due to the ^{27}Al(n, γ)^{28}Al reaction and a 6080 keV prompt gamma-ray peak caused by the ^{89}Y(n, γ)^{90}Y reaction were clearly observed. The background due to scattered neutrons from each sample was mainly attributed to the 2223 keV capture gamma-rays from the ^{1}H(n,γ)^{2}H reaction in the neutron shields of ^{6}LiH and/or borated polyethylene blocks. The main part of decay gamma-ray background from the ^{241}Am sample was observed below 1 MeV.

[Figure 11 about here.]

Correction of undetected events below the threshold level of signal processing (< 200 keV) was done by extrapolating the PH spectrum to lower energies. The PH spectrum was fitted by an exponential function from 200 keV to 600 keV, and the extrapolation of the PH spectrum below the threshold level (< 200 keV) was made. In comparison to flat extrapolation of the PH spectrum, the uncertainties due to the extrapolation were estimated. Consequently, the uncertainties were 2.7% and 1.6% for the PH spectra on ^{241}Am and ^{197}Au, respectively.

Two-dimensional data of TOF and PH spectra were reduced into one-dimensional TOF data of the weighted sum ($\sum_I W(I)S(I)$) that is proportional to the capture yield. **Figure 12** represents the weighted sum TOF spectra of the ^{241}Am, dummy, blank and ^{208}Pb. These weighted sum TOF spectra were normalized with the number of incident proton beam pulses. A peak located at 3×10^5 ch is due to the ^{241}Am first resonance (0.31 eV). Neutron resonances of the ^{241}Am

were clearly observed in the figure down to 10^4 ch , which is equivalent to a neutron energy of 260 eV. The broad peak around 2×10^6 ch is due to the neutron bump thermalized in the liquid hydrogen in the moderator. Furthermore, a neutron resonance peak of the ^{89}Y (2.6 keV) appeared at 3.5×10^3 ch. To evaluate the amount of Y_2O_3 in the ^{241}Am and the dummy samples, peak areas of this resonance were used.

[Figure 12 about here.]

Dead time correction

Dead time corrections were made for these weighted TOF spectra with extended dead-time model using a dead time of 5.67 ±0.04 μs per event. **Figure 13** illustrates the dead time corrections of the weighted TOF spectra of the ^{241}Am and the dummy samples. The dead time corrections at neutron resonance peaks of the ^{241}Am were 4.5% at the first resonance (2.9×10^5 ch, 0.31 eV) and 11% at the third resonance (2.1×10^5 ch, 1.27 eV). At the thermal energy, the dead time correction factor was 1.01. The uncertainties of the correction were deduced using the uncertainty of the dead time per event. The deduced uncertainties were less than 0.1% at the thermal energy.

[Figure 13 about here.]

Background subtraction

The following backgrounds were subtracted from the weighted TOF spectrum of the ^{241}Am sample: (1) the background due to aluminum container and Y_2O_3 included in the ^{241}Am sample; (2) the background due to scattered neutrons from the ^{241}Am sample; (3) the background caused by frame overlap neutrons, (4) the constant background due to decay gamma-rays. The background component of aluminum container and Y_2O_3 was estimated from the weighted TOF spectrum of the dummy sample considering difference of the amount of Y_2O_3 between the ^{241}Am and the dummy samples. The peak areas of the 2.6 keV resonance of ^{88}Y in the

weighted TOF spectra were taken into consideration for the amount estimation. In order to estimate the background due to scattered neutrons from the ^{241}Am sample, ^{208}Pb measurement was used. Sample-independent background, which is represented by the weighted TOF spectrum of blank, was subtracted from the weighted TOF spectrum of ^{208}Pb, and the background due to the scattered neutrons by the ^{208}Pb sample was determined. Then, the background due to scattered neutrons by the ^{241}Am sample was estimated on the assumption that the background is changed in proportion to the product of the neutron scattering cross section and the amount of target nuclei. The backgrounds caused by frame overlap neutrons and decay gamma-rays were estimated by fitting the weighted TOF spectra in the TOF region from 37 to 40 ms by using the following function:

$$f(t) = y_0 + a \exp\left(-\frac{t - 37\,ms}{t_1}\right), \tag{7}$$

where y_0, a, t_1 are fitting parameters. The fitted function was moved back in time by 40 ms. **Figure 14** indicates the fitting region and the determined background due to frame overlap neutrons and decay gamma-rays. The background component of decay gamma-rays is time-independent. Therefore, the determined y_0 includes the background due to decay gamma-rays. In the frame overlap background subtraction, the contribution from the isotopic impurity of ^{239}Pu in the ^{241}Am sample was estimated to be less than 0.1% by considering the isotopic ratio and the capture and fission cross sections of ^{239}Pu. In the similar way, background subtraction from the weighted TOF spectrum of the ^{197}Au was made.

[Figure 14 about here.]

Correction for the neutron self-shielding and multiple-scattering effects

The corrections for the neutron self-shielding and multiple-scattering effects in the ^{241}Am and ^{197}Au samples were made by using the PHITS code[47]. The dimension and weight of the samples were taken into account in the calculation. The correction for neutron self-shielding and multiple-scattering was made in the same way as boron data analysis described above. **Figures**

15 and **16** show the determined correction factors of the ^{241}Am and ^{197}Au samples, respectively. As shown in **Figures 15** and **16**, the correction factors are not so large The values were 0.3% and 2.4% for the ^{241}Am and ^{197}Au samples, respectively. In this paper, enough large uncertainties of the corrections (10%) were assumed as a rough estimation. The deduced uncertainties were 0.03% for the ^{241}Am sample and 0.24% for the ^{197}Au sample. These values are enough small comparison to other uncertainties.

[Figure 15 about here.]

[Figure 16 about here.]

Correction for the fission reaction of ^{241}Am

The correction for the fission reaction of ^{241}Am was made assuming that the multiplicity [Gamma rays/Fission] of fission reaction gamma-rays is 7.0 according to the study of Verbeke *et al.*[50]. Then, the correction factor f_{MP} for the fission reaction was derived as follows:

$$f_{\mathrm{MP}} = \frac{\sigma_{\mathrm{capture}}}{\sigma_{\mathrm{capture}} + \sigma_{\mathrm{fission}} \times \frac{MP_{\mathrm{fission}}}{MP_{\mathrm{capture}}}}, \tag{8}$$

where $\sigma_{\mathrm{capture}}$ and $\sigma_{\mathrm{fission}}$ are capture and fission cross sections of ^{241}Am, MP_{capture} and MP_{fission} are the gamma-ray multiplicities of the capture and fission reactions. The cross section data used for the correction were taken from JENDL-4.0[2]. Jandel *et al.* adopted the gamma-ray multiplicity of 4 for the ^{241}Am(n,γ) reaction[30]. Typically, neutron capture gamma-ray multiplicities vary between 1 to 6 with an average value about 3.5. In this study, the capture gamma-ray multiplicity was assumed to be 3.5. The derived correction factors were shown in **Fig. 17**. Contribution of the corrections to the capture cross section was less than 1% at thermal neutron energy. In this paper, enough large uncertainties of the corrections (10%) were assumed as a rough estimation. The estimated uncertainty was less than 0.1% and enough small comparison to other uncertainties.

[Figure 17 about here.]

3.3. Results and discussion

The neutron capture cross sections of ^{241}Am were obtained by dividing the background-subtracted ^{241}Am TOF spectrum by the incident neutron spectrum. The thermal neutron capture cross section of ^{241}Am was derived as 707 ± 29 b. The following uncertainties were taken into account for the capture cross section: (1) the statistical uncertainties of measured TOF spectra; (2) the uncertainty due to the standard capture cross section of ^{197}Au at the thermal energy (0.14%)[51]; (3) the uncertainty of the sample mass for the ^{241}Am sample; (4) the uncertainty caused by the weighting functions; (5) the uncertainties caused by the corrections for the dead time; (6) the uncertainties from the corrections for the neutron self-shielding and multiple-scattering effects for each sample; (7) the uncertainties due to the extrapolations of the capture gamma-ray PH spectrum for PHWT; (8) the uncertainty due to the correction for the fission reaction. The details of these uncertainties at the thermal energy were summarized in **Table 3**.

[Table 3 about here.]

Figure 18 shows the present results. The evaluated cross sections of JENDL-4.0[40] and JEFF-3.2[41] are also shown. The uncertainties of the determined cross sections were illustrated in **Fig. 19**. In the thermal energy region, JENDL-4.0(684 ± 39 b) is smaller than the present results by 3.3% but agrees within the uncertainties, and JEFF-3.2 (748b) is larger by 5.5%. **Table 4** compares the present results with the previous measurements on the thermal neutron capture cross sections ($\sigma_{0,\mathrm{g+m}}$) of ^{241}Am, where the thermal neutron capture cross sections to the ground state of ^{242}Am ($\sigma_{0,\mathrm{g}}$) measured by the activation methods were evaluated using the branching ratio of 0.914 ± 0.007 determined by Fioni *et al.*[26]. By comparing the measured data in the last decade, the previous data except for the result of Belgya *et al.*[31] were in good agreement with the present result within their uncertainties.

[Figure 18 about here.]

[Figure 19 about here.]

[Table 4 about here.]

Fraval *et al.*[34] measured the capture cross sections of ^{241}Am in the neutron energy region from the thermal energy to 320 eV using the neutron time-of-flight facility at the European Organization for Nuclear Research. They used a pair of C_6D_6 liquid scintillation detectors for capture gamma-ray detection. The amount of ^{241}Am sample used for the experiments was quantified with an uncertainty of 2.2% by the calorimetric method. The thermal neutron capture cross section ($\sigma_{0,g+m}$) of ^{241}Am was reported to be 678 ± 32 b. The uncertainty at the thermal energy mainly came from signal-to-background ratio. The result of Fraval *et al.* is 4.1% smaller than the present results.

Lampoudis *et al.*[19] performed neutron transmission and capture cross section measurements of ^{241}Am in the neutron energy region from the thermal neutron to 110 eV using the Geel Electron Linear Accelerator (GELINA). They measured the amount of an ^{241}Am sample with the uncertainty of 0.37% by calorimetric measurements. X-ray radiography was applied to determine the diameter of the ^{241}Am sample (22.345 ± 0.030 mm), resulting in good accuracy. The transmission measurements were performed at a flight path of 25 m with a Li-glass scintillation detector (NE905) having a thickness of 12.7 mm. The capture measurements were carried at a 12.5 m measurement station with a pair of C_6D_6 liquid scintillation detectors, and the PHWT was applied. Measured capture cross sections of ^{241}Am were normalized based on the combined analysis of transmission and capture data for the 0.31, 0.57 and 1.27 eV resonances of ^{241}Am. The thermal neutron capture cross section ($\sigma_{0,g+m}$) of ^{241}Am was determined to be 750 ± 35 b. Their result is 5.9% larger than the present results but agrees within the uncertainties.

Genreith *et al.*[32] measured the thermal neutron capture cross sections to the ground state of ^{242}Am by the activation method at the FRM II reactor. Two ^{241} Am samples with activities of 3.83 ± 0.03 and 4.66 ± 0.04 MBq were irradiated by cold neutrons. Decay gamma-rays from the irradiated ^{241}Am samples were measured with a n-type HPGe detector having a 60% relative efficiency. The thermal neutron capture cross section of each sample ($\sigma_{0,g}$) to the ground state of each sample was derived to be 663 ± 29 and 650 ± 28 b, respectively. Then they reported

the thermal neutron capture cross sections ($\sigma_{0,g+m}$) of ^{241}Am to be 725 ± 34 and 711 ± 28 b using the branching ratio measured by Fioni *et al.*[26]. The results of Genreith *et al*. are in good agreement with the present results.

Jandel *et al.*[30] measured the neutron capture cross sections of ^{241}Am in the neutron energy region from 0.0253 eV to 320 keV with the detector for advanced neutron capture experiments (DANCE) at the Los Alamos Neutron Science Center. An ^{241}Am sample with a weight of 219 ± 1 μg determined by counting alpha-particles was used for the measurements. Capture gamma-rays emitted from the ^{241}Am sample were measured with 4π BaF_2 arrays located on the 20.2 m neutron flight path. They reported the thermal neutron capture cross section ($\sigma_{0,g+m}$) of ^{241}Am to be 665 ± 33 b, which is 5.9% smaller than the present results but agrees within the uncertainties.

Belgya *et al.*[31] measured the capture cross section ($\sigma_{0,g}$) of ^{241}Am by measuring X-rays from the decay product of ^{242}Pu at the Budapest Research Reactor. It is noted that uncertainties ascribed to X-ray emission probabilities of 103.4 keV and 99.5 keV from ^{242}Pu were the most dominant uncertainty component. The discrepancy of the thermal capture cross sections of ^{241}Am might be caused by these X-ray emission probabilities. Additionally, Mizuyama *et al.*[52] reported that the discrepancy can be improved by their new developed correction method considering an influence by the resonances near and below a Cd cut-off energy (0.5 eV).

4. Conclusions

The neutron total cross sections and neutron capture cross sections of ^{241}Am were measured by the TOF method with the Li-Glass detectors and the cluster-Ge detectors of ANNRI in J-PARC. The neutron total cross section was deduced in the neutron energy region from 4 meV to 2 eV and the obtained thermal total cross section was 730 ± 21 b. Compared with the value obtained in this work, the JENDL-4.0 is 4.2% smaller, and the JEFF-3.2 is 4.7% larger. The neutron capture cross sections of ^{241}Am were deduced in neutron energies range from 10 meV to 100 eV. The thermal neutron capture cross sections was derived as 707±29 b by using the PHWT

using the thermal neutron capture cross section of ^{197}Au in JENDL-4.0. The obtained neutron total and capture cross sections were consistent. These results can contribute to improving the accuracy of nuclear data on ^{241}Am.

Acknowledgments

The author would like to thank the accelerator and technical staff at J-PARC for operation of the accelerator and the neutron production target and for the other experimental supports. Present study includes the result of “Research and Development for accuracy improvement of neutron nuclear data on minor actinides” entrusted to the Japan Atomic Energy Agency by the Ministry of Education, Culture, Sports, Science and Technology of Japan (MEXT).

Disclosure statement

No potential conflict of interest was reported by the authors.

References

[1] Iwamoto H, Nishihara K, Sugawara T, Tsujimoto K. Sensitivity and uncertainty analysis for an accelerator-driven system with JENDL-4.0. J. Nucl. Sci. Technol. 2013;50:856-862.

[2] Shibata K, Iwamoto O, Nakagawa T, Iwamoto N, Ichihara A, Kunieda S, Chiba S, Furukawa K, Otuka N, Ohsawa T, Murata T, Matsunobu H, Zukaran A, Kameda S, Katakura J. JENDL-4.0: A new library for nuclear science and technology. J Nucl Sci Technol. 2011;48:1-30.

[3] Salvatore M, Jacqmin R. UNCERTAINTY AND TARGET ACCURACY ASSESSMENT FOR INNOVATIVE SYSTEMS USING RECENT COVARIANCE DATA EVALUATIONS. WPEC-26, OECD NEA(2008).

[4] Harada H, Iwamoto O, Iwamoto N, Kimura A, Terada K, Nakao T, Nakamura S, Mizuyama K, Igashira M, Katabuchi T, Sano T, Takahashi Y, Takamiya K, Pyeon C H, Fukutani S, Hori J, Yagi T, Yashima H. Accuracy Improvement of Neutron Nuclear Data on Minor Actinides. In Proceedings of the 15’th International Sym-

posium on Capture Gamma-Ray Spectroscopy and Related Topics (CGS 15); 2014 August 25-29; Dresden, Germany. EPJ Web of Conferences 93.

[5] Harada H, Iwamoto O, Iwamoto N, Kimura A, Terada K, Nakao T, Nakamura S, Mizuyama K, Igashira M, Katabuchi T, Sano T, Takahashi Y, Takamiya K, Pyeon C H, Fukutani S, Hori J, Yagi T, Yashima H. Research and development for accuracy improvement of neutron nuclear data on minor actinides. In Proceedings of the International Conference on Nuclear Data for Science and Technology (ND2016); 2016 September 11-16; Bruges, Belgium. EPJ Web of Conferences 2017;146:11001.

[6] Nakao T, Terada K, Kimura A, Nakamura S, Iwamoto O, Harada T, Katabuchi T, Igashira M, Hori J. Developments of a new data acquisition system at ANNRI. In Proceedings of the International Conference on Nuclear Data for Science and Technology (ND2016); 2016 September 11-16; Bruges, Belgium. EPJ Web of Conferences 2017;146:03021.

[7] Terada K, Nakao T, Kimura A, Nakamura S, Iwamoto O, Harada T, Takamiya K, Hori J. Technical developments for accurate determination of amount of samples used for TOF measurements. In Proceedings of the International Conference on Nuclear Data for Science and Technology (ND2016); 2016 September 11-16; Bruges, Belgium. EPJ Web of Conferences 2017;146:03019.

[8] Shibahara S, Hori J, Takamiya K, Fujii S, Fukutani S, Sano T, Harada H. High precision analysis of isotopic composition for samples used for nuclear cross-section measurements. In Proceedings of the International Conference on Nuclear Data for Science and Technology (ND2016); 2016 September 11-16; Bruges, Belgium. EPJ Web of Conferences 2017;146:03028.

[9] Hirose K, Furutaka K, Hara K, Harada H, Kimura A, Kin T, Kitatani F, Koizumi M, Nakamura S, Oshima M, Toh Y, Igashira M, Katabuchi T, Mizumoto M, Kamiyama T, Kino K, Kiyanagi Y, Hori J. Cross-Section Measurement of ^{237}Np(n,γ) from 10 meV to 1 keV at Japan Proton Accelerator Research Complex J. Nucl. Sci. Technol. 2013;50:188-200.

[10] Harada H, Ohta M, Kimura A, Furutaka K, Hirose K, Hara K, Kin T, Kitatani F, Koizumi M, Nakamura S, Oshima M, Toh Y, Igashira M, Katabuchi T, Mizumoto M, Kino K, Kiyanagi Y, Fujii T, Fukutani S, Hori J, Takamiya K. Measurements of ^{241}Am(n,γ) at J-PARC/MLF/ANNRI. Nuclear Data Sheets 2014;119:61-64.

[11] Kimura A, Fujii T, Fukutani S, Furutaka K, Goko S, Hara K, Harada H, Hirose K, Hori J, Igashira M, Kamiyama T, Katabuchi T, Kin T, Kino K, Kitatani F, Kiyanagi Y, Koizumi M, Mizumoto M, Nakamura S, Ohta M, Oshima M, Takamiya K, Toh Y. Neutron-Capture Cross-Sections of ^{244}Cm and ^{246}Cm Measured with an Array of Large Germanium Detectors in the ANNRI at J-PARC/MLF. J. Nucl. Sci. Technol. 2011;49:708-724.

[12] Mendoza E, Cano-Ott D, Guerrero C, Berthoumieux E, Abbondanno U, Aerts G, Álvarez-Velarde F, Andriamonje S, Andrzejewski J, Assimakopoulos P, Audouin L, Badurek G, Balibrea J, Baumann P, Bečvář F, Belloni F, Calviño F, Calviani M, Capote R, Carrapiço C, Carrillo de Albornoz A, Cennini P, Chepel V, Chiaveri E, Colonna N, Cortes G, Couture A, Cox J, Dahlfors M, David S, Dillmann I, Dolfini R, Domingo-Pardo C, Dridi W, Duran I, Eleftheriadis C, Ferrant L, Ferrari A, Ferreira-Marques R, Fitzpatrick L, Frais-Koelbl H, Fujii K, Furman W, Goncalves I, González-Romero E, Goverdovski A, Gramegna F, Griesmayer E, Gunsing F, Haas B, Haight R, Heil M, Herrera-Martinez A, Igashira M, Isaev S, Jericha E, Käppeler F, Kadi Y, Karadimos D, Karamanis D, Ketlerov V, Kerveno M, Koehler P, Konovalov V, Kossionides E, Krtička M, Lampoudis C, Leeb H, Lindote A, Lo Meo S, Lopes I, Lossito R, Lozano M, Lukic S, Marganiec J, Marques L, Marrone S, Martínez T, Massimi C, Mastinu P, Mengoni A, Milazzo P, M, Moreau C, Mosconi M, Neves F, Oberhummer H, O'Brien S, Oshima M, Pancin J, Papachristodoulou C, Papadopoulos C, Paradela C, Patronis N, Pavlik A, Pavlopoulos P, Perrot L, Pigni M, T, Plag R, Plompen A, Plukis A, Poch A, Praena J, Pretel C, Quesada J, Rauscher T, Reifarth R, Rubbia C, Rudolf G, Rullhusen P, Salgado J, Santos C, Sarchiapone L, Savvidis I, Stephan C, Tagliente G, Tain J, L, Tassan-Got L, Tavora L, Terlizzi R, Vannini G, Vaz P, Ventura A, Villamarin D, Vicente M, C, Vlachoudis V, Vlastou R, Voss F, Walter S, Wendler H, Wiescher M, Wisshak K. Measurement and analysis of the ^{243}Am neutron capture cross section at the n_TOF facility at CERN. Phys. Rev. C. 2014;90:034608.

[13] Adamchuk Ju V, Gerasimov V F, Efimov B V, Zenkevich V S, Mostovoy V I, Pevzner M I, Tsitovich A P, Chernyshov A A, Moskalev S S. The fission and total cross-sections measurement for heavy elements isotopes by monochromatic neutrons using mechanical selector. In Proceedings of the International Conference on Peaceful Uses of Atomic Energy; 1955 August 8; Geneva, Schweizerische. Vol.4, p.259.

[14] Slaughter G G, Block R C, Harvey J A. High-Resolution Total Cross Section Measurements on ^{237}Np and ^{241}Am using the ORNL Fast Chopper. Am. Phys. Soc. 1961;6:70.

[15] Derrien H, Lucas B. The total cross section and the fission cross section of ^{241}Am in the resonance region. In Proceedings of the International Conference on nuclear cross sections and technology; 1975 March 3-7; Washington, D.C., USA. Vol.2, p.637.

[16] Belanova T S, Kolesov A G, Nikolaev V M, Safonv V A, Gabeskiriya V Y, Poruchikov V A, Gudkov O M. Parameters of the Neutron Resonances of ^{241}Am in the Energy Range from 8 to 30 eV. Sov. At. Energy. 1975;38:29.

[17] Kalabin S M, Artamonov V S, Ivanov R N, Rukolaine G V, Velanova T S, Kolesov A G. Total Neutron Cross Section and Neutron Resonance Parameters of ^{241}Am In the Energy Range 0.004-30 eV. Sov. At. Energy. 1976;40:303.

[18] Phillips T W, Howe R E. Total neutron cross section for Americium-241. Nuclear Science and Engineering. 1979;69:375-377.

[19] Lampoudis C, Kopecky S, Bouland O, Gunsing F, Noguerre G, Plompen A J M, Sage C, Schillebeeckx P, Wynants R. Neutron transmission and capture cross section measurements for ^{241}Am at the GELINA facility. The European Physical Journal Plus. 2013;128:86.

[20] Pomerance H. Absorption Cross Sections For Long-Lived Fission-Product Zr93, Am241, And Enriched Stable Platinum Isotopes, in Physics Division Semiannual Progress Report (ORNL). 1955;5055.

[21] Bak M A, Krivokhatskii A S, Petrzhak K A, Petrov Yu G, Romanov Yu F, Shlyamin E A. Cross sections and resonance integrals for capture and fission in long-lived americium isotopes. Atomnaya Energiya. 1967;23:316.

[22] Dovbenko A G, Ivanov V I, Kolesov V E, Tolstikov V A. Am-241 radiative neutron capture. Centr po Jadernym Dannym, Obninsk. 1969;6:42.

[23] Harbour R M, Mac Murdo K W, Crosson F J. Thermal-Neutron Capture Cross Sections and Capture Resonance Integrals of Americium-241.Nuclear Science and Engineering. 1973;50:364.

[24] Gavrilov V D, Goncharov V A, Ivaneko V V, Kustov V N, Smirnov V P. Thermal cross sections and resonance

integrals of fission and capture of Am-241, Am-243, Bk-249, and Cf-249. Atomnaya Energiya. 1976;41:808.

[25] Shinohara N, Hatsukawa Y, Hata K, Kohno N. Radiochemical determination of Neutron capture cross section of ^{241}Am. Journal of Nuclear Science and Technology. 1997;34:613-621.

[26] Fioni G, Cribier M, Marie F, Aubert M, Ayrault S, Bolognese T, Cavedon J M, Chartier F, Deruelle O, Doneddu F, Faust H, Gaudry A, Gunsing F, Leconte Ph, Lelievre F, Martino J, Oliver R, Pluquet A, Röttger S, Spiro M, Veyssiere C. Incineration of ^{241}Am induced by thermal neutrons. Nuclear Physics A. 2001;693:546-564.

[27] Maidana N L, Dias M S, Foskinas M F. Measurement of the thermal neutron capture cross section and resonance integral of Am-241. Radiochimica Acta. 2001;89:419-423.

[28] Bringer O, AlMahamid I, Chabod S, Chartier F, Dupont E, Letourneau A, Mutti P, Oriol L, Panebianco S Veyssière C. Measurements of thermal fission and capture cross sections of minor actinides within the Mini-INCA project. Proceedings of the International Conference onNuclear Data for Science and Technology 2007; 2007 April 22-28; Nice, France. p.619-622.

[29] Nakamura S, Ohta S, Harada H, Fujii T, Yamana H. Thermal-Neutron Capture Cross Section and Resonance Integral of Americium-241. Journal of Nuclear Science and Technology. 2007;44:1500-1508.

[30] Jandel M, Bredeweg T A, Bond E M, Chadwick M B, Clement R R, Couture A, O'Donnell J M, Haight R C, Kawano T, Reifarth R, Rundberg R S, Ullmann J L, Vieira D J, Wilhelmy J B, Wouters J M, Agvaanluvsan U, Parker W E, Wu C Y, Becker J A. Neutron capture cross section of ^{241}Am. Phys. Rev. C. 2008;78:034609.

[31] Belgya T, Szentmiklosi L, Kis Z, Nagy N M, Konya J. Measurement of ^{241}Am ground state radiative neutron capture cross section with cold neutron beam. IAEA Report INDC (HUN). 2012;0037.

[32] Genreith C, Rossbach M, Révay Zs, Kudejova P. Determination of (n,γ) Cross Sections of ^{241}Am by Cold Neutron Activation. Nuclear Data Sheets. 2014;119:69-71.

[33] Lampoudis C, Kopecky S, Bouland O, Gunsing F, Noguere G, Plompen A J M, Sage C, Schillebeeckx P, Wynants R. Neutron transmission and capture cross section measurements for ^{241}Am at the GELINA facility. The European Physical Journal Plus. 2013;128:86.

[34] Fraval K, Gunsing F, Altstadt S, Andrzejewski J, Audouin L, Barbagallo M, Bécares V, Bečvćř F, Belloni F,

Berthoumieux E, Billowes J, Boccone V, Bosnar D, Brugger M, Calviani M, Calviño F, Cano-Ott D, Carrapiç C, Cerutti F, Chiaveri E, Chin M, Colonna N, Cortés G, Cortés-Giraldo M. A, Diakaki M, Domingo-Pardo C, Duran I, Dressler R, Dzysiuk N, Eleftheriadis C, Ferrari A, Ganesan S, García A R, Giubrone G, Gomez-Hornillos M. B, Gonçalves I. F, Gonzalez-Romero E, Griesmayer E, Guerrero C, Gurusamy P, Hernandez-Prieto A, Jenkins D. G, Jericha E, Kadi Y, Kappeler F, Karadimos D, Kivel N, Koehler P, Kokkoris M, Krtička M, Kroll J, Lampoudis C, Langer C, Leal-Cidoncha E, Lederer C, Leeb H, Leong L. S, Losito R, Mallick A, Manousos A, Marganiec J, Martinez T, Massimi C, Mastinu P. F, Mastromarco M, Meaze M, Mendoza E, Mengoni A, Milazzo P. M, Mingrone F, Mirea M, Mondalaers W, Paradela C, Pavlik A, Perkowski J, Plompen A, Praena J, Quesada J. M, Rauscher T, Reifarth R, Riego A, Robles M. S, Roman F, Rubbia C, Sabaté-Gilarte M, Sarmento R, Saxena A, Schillebeeckx P, Schmidt S, Schumann D, Tagliente G, Tain J. L, Tarrío D, Tassan-Got L, Tsinganis A, Valenta S, Vannini G, Variale V, Vaz P, Ventura A, Versaci R, Vermeulen M. J, Vlachoudis V, Vlastou R, Wallner A, Ware T, Weigand M, Weis C, Wright T, Žugec P. Measurement and analysis of the ^{241}Am(n,γ) cross section with liquid scintillator detectors using time-of-flight spectroscopy at the n_TOF facility at CERN. Phys. Rev. C. 2014;89:044609.

[35] Hirose K, Nishio K, Makii H, Nishinaka I, Ota S, Nagayama T, Tamua T, Goto S, Andreyev A N, Vermeulen M J, Gilespied S, Barton C, Kimura A, Harada H, Meigo S, Chiba S. Simultaneous measurement of neutron-induced fission and capture cross sections for ^{241}Am at neutron energies below fission threshold. Nuclear Instruments and Methods in Physics Research Section A. 2017;856:133-138.

[36] Žerovnik G, Schilleveeckx P, Cano-Ott D, Jandel M, Hori J, Kimura A, Rossbach M, Letourneau A, Noguere G, Leconte P, Sano T, Kellett M A, Iwamoto O, Ignatyuk A V, Cabellos O, Genreith C, Harada H. Improving nuclear data accuracy of ^{241}Am and 237Np capture cross sections. In Proceedings of the International Conference on Nuclear Data for Science and Technology (ND2016); 2016 September 11-16; Bruges, Belgium. EPJ Web of Conferences 2017;146:11035.

[37] Maekawa F, Harada M, Oikawa K, Teshigawara M, Kai T, Meigo S, Ooi M, Sakamoto S, Takeda H, Futakawa M, Kato T, Ikeda Y, Watanabe N, Kamiyama T, Torii S, Kajimoto R, Nakamura M. 2010. First neutron production utilizing J-PARC pulsed spallation neutron source JSNS and neutronic performance demonstrated.

Nuclear Instruments and Methods in Physics Research Section A. 2010;620: 159165.

[38] Igashira M, Kiyanagi Y, Oshima M. Nuclear data study at J-PARC BL04. Nuclear Instruments and Methods in Physics Research Section A. 2009;600:332-334.

[39] Kino K, Furusaka M, Hiraga F, Kamiyama T, Kiyanagi Y, Furutaka K, Goko S, Harada H, Harada M, Kai T, Kimura A, Kin T, Kitatani F, Koizumi M, Maekawa F, Meigo S, Nakamura S, Ooi M, Ohta M, Oshima M, Toh Y, Igashira M, Katabuchi T, Mizumoto M. Measurement of energy spectra and spatial distributions of neutron beams provided by the ANNRI beamline for capture cross-section measurements at the J-PARC/MLF. Nuclear Instruments and Methods in Physics Research Section A. 2011;626:58-66.

[40] JENDL-4.0 data file for ^{241}Am (MAT=9543), evaluated by Iwamoto N (2010).

[41] JEFF-3.2 data file for ^{241}Am (MAT=9543), evaluated by CEA/NRG/IRMM collaboration (2014).

[42] ENDF/B-VII.1 data file for ^{241}Am (MAT=9543), evaluated by Kawano T and Chadwick M B (2011).

[43] Kimura A., Fujii T., Fukutani S., Furutaka K., Goko S. , HaraK. Y., Harada H., Hirose K., Hori J., Igashira M., Kamiyama T., Katabuchi T., Kin T., Kino K., Kitatani F., Kiyanagi Y., Koizumi M., Mizumoto M., Nakamura S., Ohta M., Oshima M., Takamiya K., Toh Y. Neutron-capture cross-sections of ^{244}Cm and ^{246}Cm measured with an array of large germanium detectors in the ANNRI at J-PARC/MLF. Journal of Nuclear Science and Technology 2012;49:708-724. .

[44] Kin T, Furutaka K, Goko S, Harada H, Igashira M, Kamiyama T, Katabuchi T, Kimura A, Kino K, Kitatani F, Kiyanagi Y, Koizumi M, Mizumoto M, Nakamura S, Ota M, Oshima M, Toh Y. Development of a 4*pi* germanium spectrometer for nuclear data measurements at J-PARC. In Proceedings of the International Conference on 2009 IEEE Nuclear Science Symposium and Medical Imaging; 2009 October 25-31, Orland, USA. pp. 2531.

[45] Macklin R L, Gibbons J H. Capture-cross-section studies for 30-220 keV neutrons using a new technique. Phys. Rev. 1967;159:1007-1015.

[46] JENDL-4.0 data file for ^{10}B (MAT = 525), evaluated by Chiba S (2010).

[47] Sato T, Niita K, Matsuda N, Hashimoto S, Iwamoto Y, Noda S, Ogawa T, Iwase H, Nakashima H, Fukahori T, Okumura K, Kai T, Chiba S, Furuta T, Sihver L. Particle and Heavy Ion Transport Code System PHITS

Version 2.52. J. Nucl. Sci. Technol. 2013;50:913-923.

[48] Allison J, Amako K, Apostolakis J, Arce P, Asai M, Aso T, Bagli E, Bagulya A, Banerjee S, Barrand G, Beck B R, Bogdanov A G, Brandt D, Brown J M C, Burkhardt H, Canal Ph, Cano-Ott D, Chauvie D, Cho K, Cirrone G A P, Cooperman G, Corts-Giraldo M A, Cosmo G, Cuttone G, Depaola G, Desorgher L, Dong X, Dotti A, Elvira V D, Folger G, Francis Z, Galoyan A, Garnier L, Gayer M, Genser K L, Grichine V M, Guatelli S, Gueye P, Gumplinger P, Howard A S, Hrivnacova I, Hwang S, Incerti S, Ivanchenko A, Ivanchenko V N, Jones F W, Jun S Y, Kaitaniemi P, Karakatsanis N, Karamitros M, Kelsey M, Kimura A, Koi T, Kurashige H, Lechner A, Lee S B, Longo F, Maire M, Mancusi D, Mantero A, Mendoza E, Morgan B, Murakami K, Nikitina T, Pandola L, Paprocki P, Perl J, Petrovic I, Pia M G, Pokorski W, Quesada J M, Raine M, Reis M A, Ribon A, Ristic Fira A, Romano F, Russo G, Santin G, Sasaki T, Sawkey D, Shin J I, Strakovsky I I, Taborda A, Tanaka S, Tome B, Toshito T, Tran H N, Truscott P R, Urban L, Uzhinsky V, Verbeke J M, Verderi M, Wendt B L, Wenzel H, Wright D H, Wright D M, Yamashita T, Yarba J, Yoshida H. Recent developments in Geant4. Nuclear Instruments and Methods in Physics Research Section A. 2016;835:186-225.

[49] JENDL-4.0 data file for ^{197}Au (MAT=7925), evaluated by Iwamoto N (2010).

[50] Verbeke J M, Hagmann C, Wright D. Simulation of Neutron and Gamma Ray Emission from Fission and Photofission. LLNL Fission Library 2.0.2. Lawrence Livermore. 2014.

[51] Carlson A D, Pronyaev V G, Smith D L, Larson N M, Zhenpeng C, Hale G M, Hambsch F J, Gai E V, Oh S Y, Badikov S A, Kawano T, Hofmann H M, Vonach H, Tagesen S. International Evaluation of Neutron Cross Section Standards. Nuclear Data Sheets. 2009;110:3125-3324.

[52] Mizuyama K, Iwamoto N, Iwamoto O. Correction of the thermal neutron capture cross section of 241Am obtained by the Westcott convention. Journal of Nuclear Science and Technology. 2017;54:74-80.

Table 1 Characteristics of the samples

Sample	^{241}Am	Dummy
Inclusion	AmO_2 +Y_2O_3	Y_2O_3
Activity [MBq]	957.4 ± 0.5	-
Weight of Y_2O_3 [mg]	46.0	66.2
Composition [%]		
^{241}Am	99.9	-
^{239}Pu	0.09	-
Diameter [mm]	10.0 ± 0.1	10.0 ± 0.1
Thickness [mm]	0.5 ± 0.1	0.5 ± 0.1

Table 2 Measuring times

Samples	Measuring time [h]
^{241}Am	41
Dummy	26
^{197}Au	5
^{10}B	5
^{208}Pb	12
Blank	9

Table 3 Details of uncertainties for the derived thermal capture cross section of ^{241}Am.

Uncertainties	[%]
Statistics	0.5
Capture cross section standard	0.1
Sample mass	0.2
Weighting function	1.0
Dead time	< 0.1
Self-shielding and multiple-scattering	
^{241}Am	< 0.1
^{197}Au	0.2
^{10}B	2.3
Extrapolation of PH spectra	
^{241}Am	2.7
^{197}Au	1.1
Fission	< 0.1
Total	4.0

Table 4 The thermal neutron capture cross sections ($\sigma_{0,g+m}$) of ^{241}Am.

Year	Thermal cross section [b]	Author
2017	707 ± 29	Present
2014	678 ± 32	Fraval *et al.*
2013	750 ± 35	Lampoudis *et al.*
2013	725 ± 34	Genreith *et al.*
2013	711 ± 28	Genreith *et al.*
2012	591 ± 35	Belgya *et al.*
2008	665 ± 33	Jandel *et al.*
2007	702 ± 25	Nakamura *et al.*
2007	705 ± 23	Bringer *et al.*
2001	672 ± 10	Maidana *et al.*
2001	696 ± 48	Fioni *et al.*
1997	853 ± 52	Shinohara *et al.*
1976	625 ± 30	Kalebin *et al.*
1976	853 ± 52	Gavrilov *et al.*
1973	612 ± 25	Harbour *et al.*
1969	654 ± 104	Dovbenko *et al.*
1967	740 ± 60	Bak *et al.*
1955	629 ± 35	Pomerance *et al.*

Figure Captions

Figure 1 Present status on total cross sections of ^{241}Am.

Figure 2 PH spectra of the ^{6}Li detector and the ^{7}Li detector.

Figure 3 Gated TOF spectra of the ^{241}Am (red) and the dummy samples (blue) measured with the ^{6}Li-glass detector and the ^{7}Li-glass detector. Solid lines show the neutron TOF spectra measured by the ^{6}Li-glass detector. Dashed lines show the gamma-ray backgrounds measured by the ^{7}Li-glass detector. The channel width was 4 ns/ch. Each TOF spectrum was normalized with the number proton beam pulses.

Figure 4 The gated neutron TOF spectra and the frame overlap background of the ^{241}Am sample. A Solid line shows the gated neutron TOF spectra measured by the ^{6}Li-glass detector. A dashed line shows the deduced frame overlap background. The channel width was 4 ns/ch.

Figure 5 The neutron transmission ratio of ^{241}Am. The channel width was 4 ns/ch.

Figure 6 The derived neutron total cross sections of ^{241}Am (red points) with comparison to the results by Adamchk[13] (Black points), the evaluated values in JENDL-4.0[40] (blue line) and JEFF-3.2[41] (black line).

Figure 7 The correction factor of the neutron self-shielding and multiple scattering in the ^{10}B sample.

Figure 8 Incident neutron energy spectrum determined by measuring the 478 keV

gamma-ray from the ^{10}B(n, $\alpha\gamma$)^{7}Li reactions.

Figure 9 A comparison between calculated and measured response functions for a ^{60}Co source. The calculated response function was normalized with the number of emitted gamma-rays. Differences of the peak areas on the 1173 and 1332 keV between the experiment and the calculation were less than 2%.

Figure 10 The calculated weighting function for the ^{241}Am sample without the normalization.

Figure 11 The PH spectra of the ^{241}Am (red), dummy (black), ^{208}Pb (blue) and ^{241}Am decay (green) measurements. These PH spectra were normalized using the number of proton beam pulses. Sample-independent background estimated from the PH spectra for the blank measurement was subtracted.

Figure 12 The weighted sum TOF spectra of the ^{241}Am, dummy, ^{208}Pb and blank (1 ch = 10 ns). These weighted sum TOF spectra were normalized with the number of proton beam pulses. Red line is the ^{241}Am, black line is the dummy, green line is the ^{208}Pb and blue line is blank.

Figure 13 The dead time corrections for the weighted TOF spectra of the the ^{241}Am and dummy measurements.

Figure 14 The background of frame overlap neutrons compared with the weighted TOF spectrum of the ^{241}Am sample.

Figure 15 The correction for neutron self-shielding and multiple-scattering on the ^{241}Am sample.

Figure 16 The correction for neutron self-shielding and multiple-scattering on the ^{197}Au sample.

Figure 17 The correction for the fission reaction of ^{241}Am.

Figure 18 The determined neutron capture cross sections of ^{241}Am.

Figure 19 The uncertainties of the derived neutron capture cross sections of ^{241}Am. A step appeared at neutron energy of 2.4 eV following a change of the TOF bin width

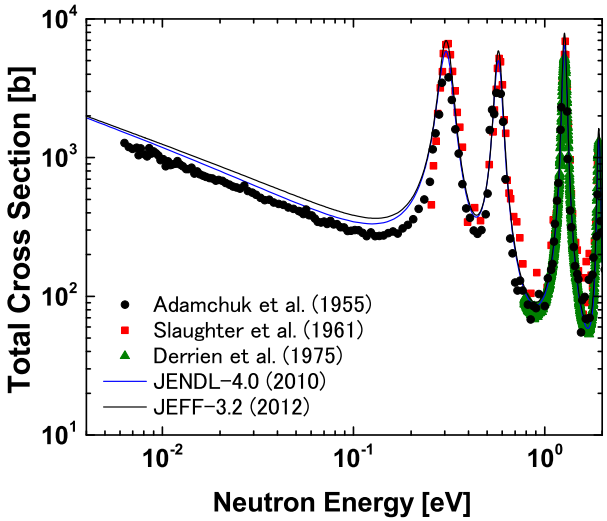

Figure 1 Present status on total cross sections of ^{241}Am.

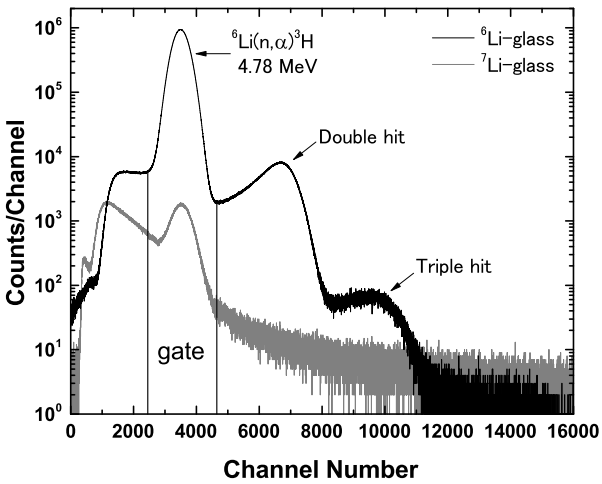

Figure 2 PH spectra of the ^{6}Li detector and the ^{7}Li detector.

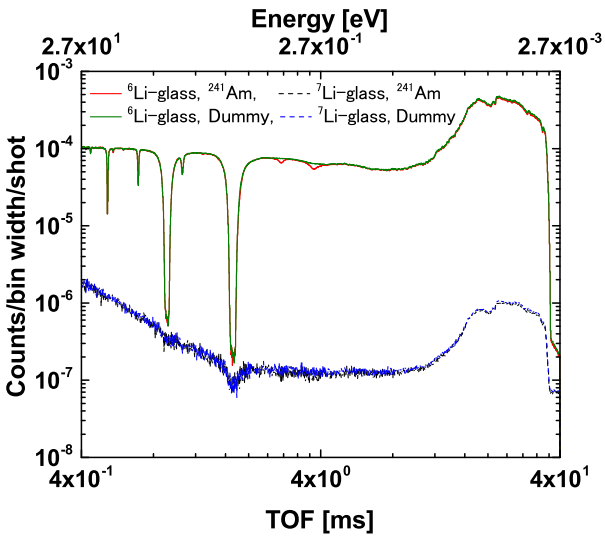

Figure 3 Gated TOF spectra of the ^{241}Am (red) and the dummy samples (blue) measured with the ^{6}Li-glass detector and the ^{7}Li-glass detector. Solid lines show the neutron TOF spectra measured by the ^{6}Li-glass detector. Dashed lines show the gamma-ray backgrounds measured by the ^{7}Li-glass detector. The channel width was 4 ns/ch. Each TOF spectrum was normalized with the number proton beam pulses.

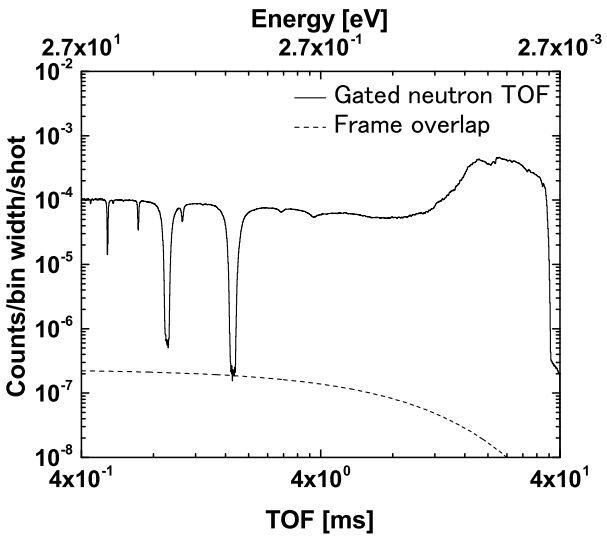

Figure 4 The gated neutron TOF spectra and the frame overlap background of the ^{241}Am sample. A Solid line shows the gated neutron TOF spectra measured by the ^{6}Li-glass detector. A dashed line shows the deduced frame overlap background. The channel width was 4 ns/ch.

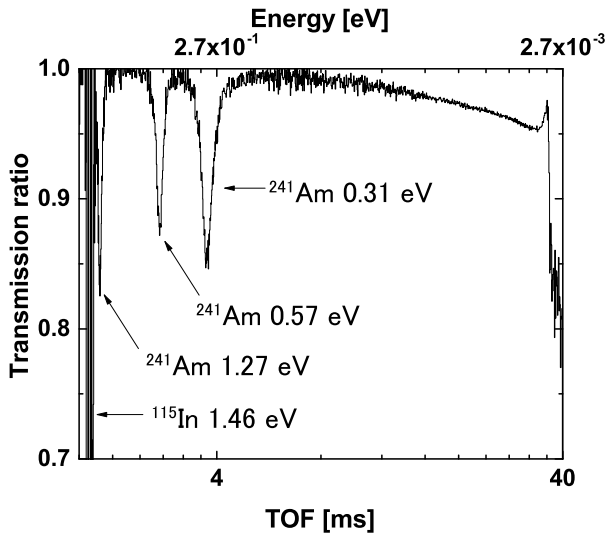

Figure 5 The neutron transmission ratio of ^{241}Am. The channel width was 4 ns/ch.

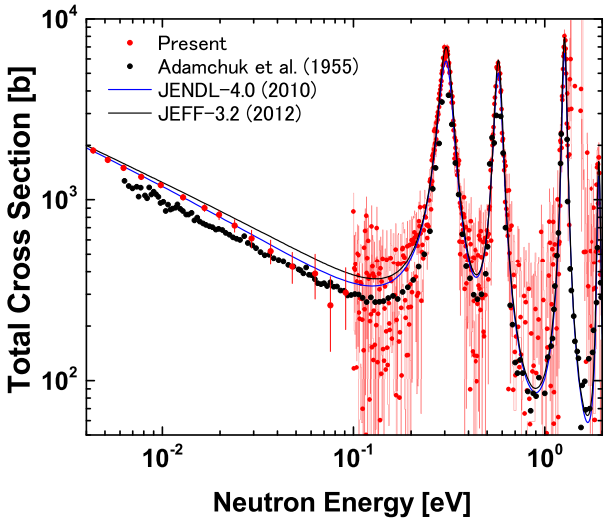

Figure 6 The derived neutron total cross sections of ^{241}Am (red points) with comparison to the results by Adamchk[13] (Black points), the evaluated values in JENDL-4.0[40] (blue line) and JEFF-3.2[41] (black line).

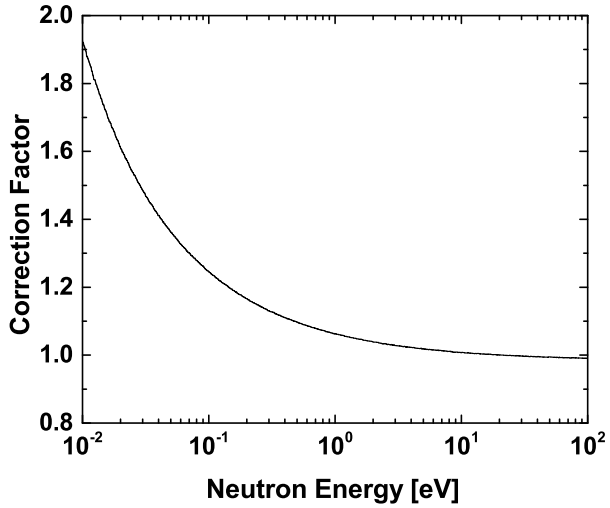

Figure 7 The correction factor of the neutron self-shielding and multiple scattering in the ^{10}B sample.

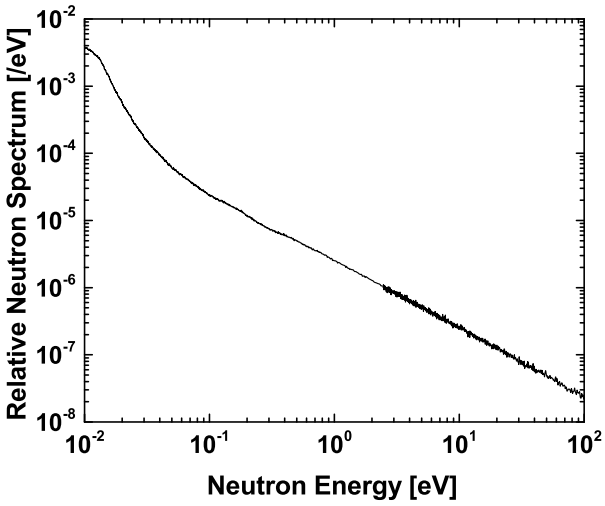

Figure 8 Incident neutron energy spectrum determined by measuring the 478 keV gamma-ray from the ^{10}B(n, $\alpha\gamma$)^{7}Li reactions.

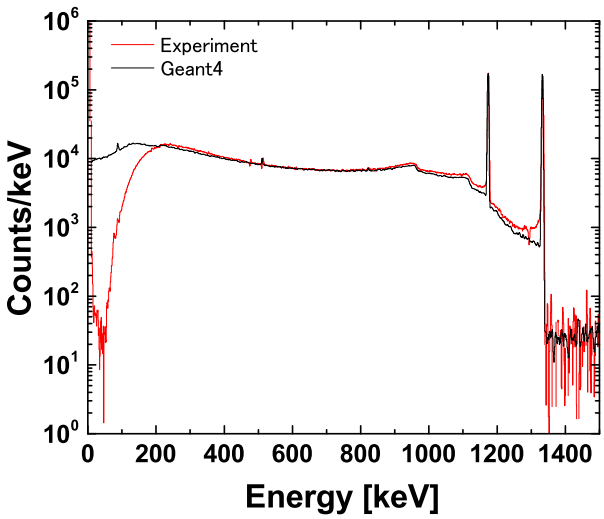

Figure 9 A comparison between calculated and measured response functions for a ^{60}Co source. The calculated response function was normalized with the number of emitted gamma-rays. Differences of the peak areas on the 1173 and 1332 keV between the experiment and the calculation were less than 2%.

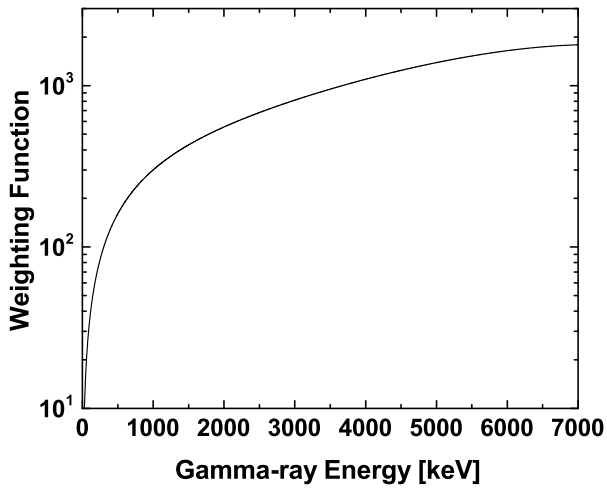

Figure 10 The calculated weighting function for the ^{241}Am sample without the normalization.

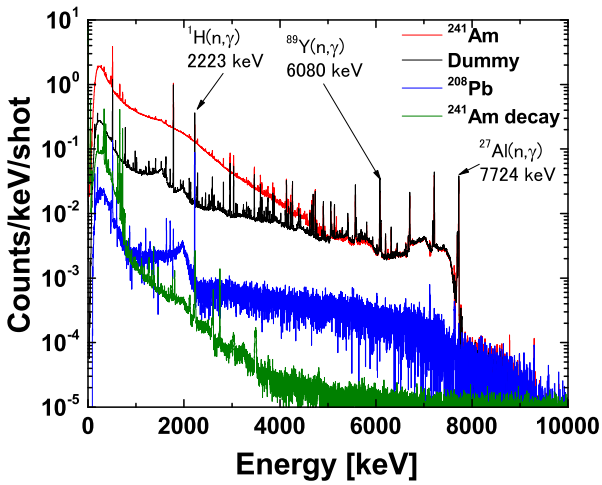

Figure 11 The PH spectra of the ^{241}Am (red), dummy (black), ^{208}Pb (blue) and ^{241}Am decay (green) measurements. These PH spectra were normalized using the number of proton beam pulses. Sample-independent background estimated from the PH spectra for the blank measurement was subtracted.

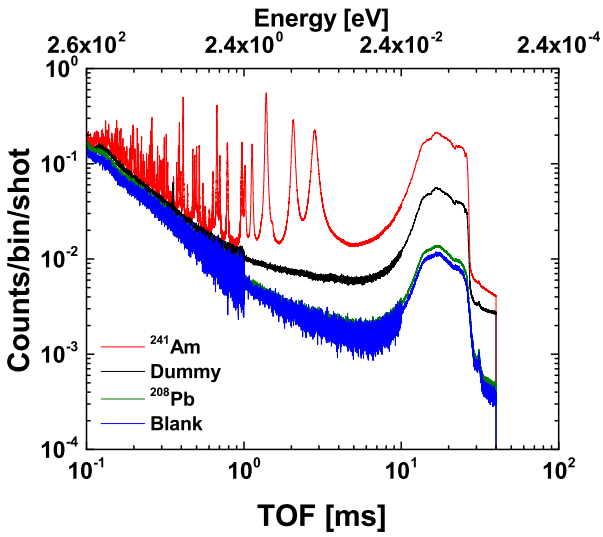

Figure 12 The weighted sum TOF spectra of the ^{241}Am, dummy, ^{208}Pb and blank (1 ch = 10 ns). These weighted sum TOF spectra were normalized with the number of proton beam pulses. Red line is the ^{241}Am, black line is the dummy, green line is the ^{208}Pb and blue line is blank.

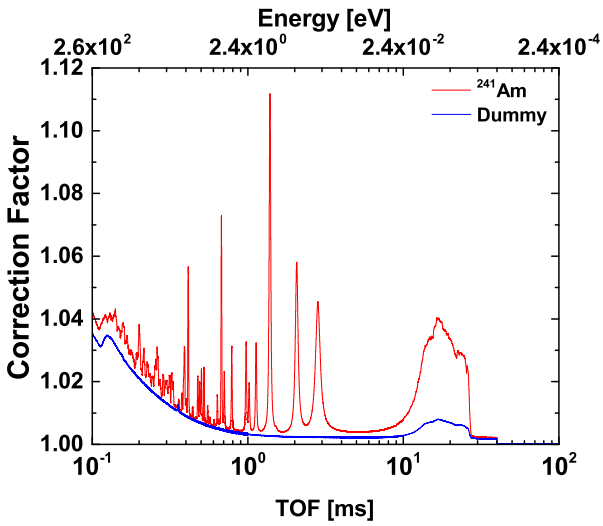

Figure 13 The dead time corrections for the weighted TOF spectra of the the ^{241}Am and dummy measurements.

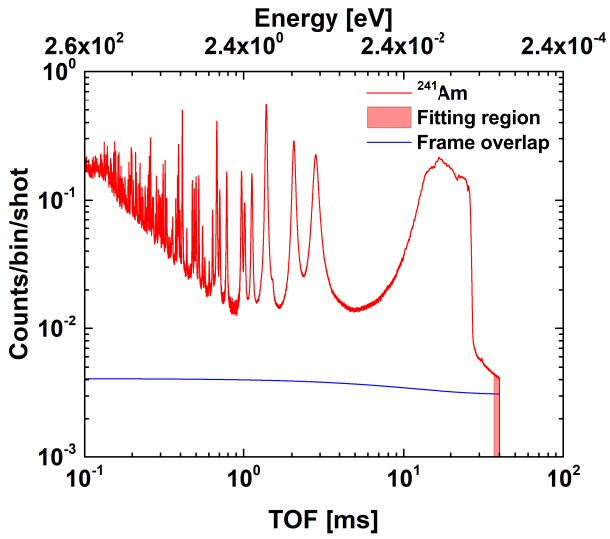

Figure 14 The background of frame overlap neutrons compared with the weighted TOF spectrum of the ^{241}Am sample.

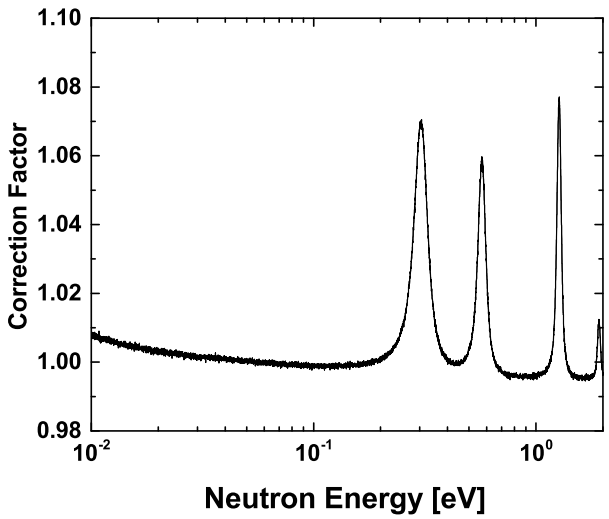

Figure 15 The correction for neutron self-shielding and multiple-scattering on the ^{241}Am sample.

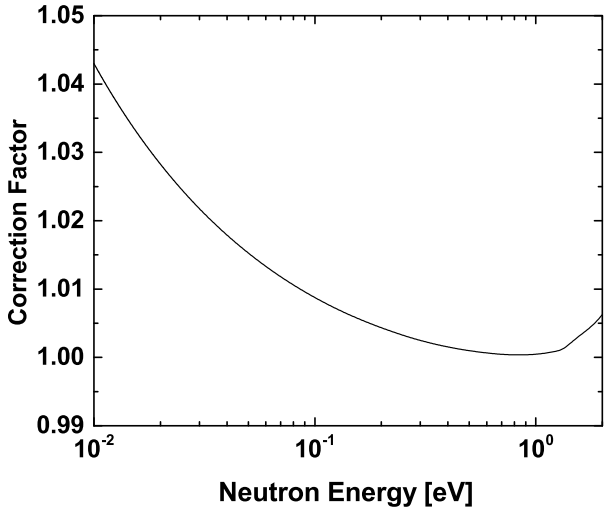

Figure 16 The correction for neutron self-shielding and multiple-scattering on the ^{197}Au sample.

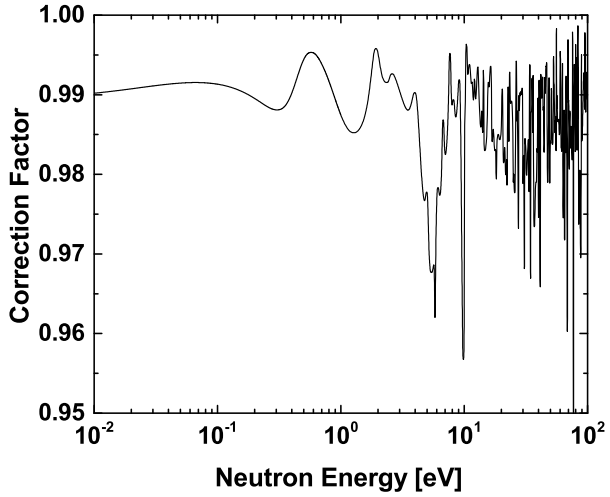

Figure 17 The correction for the fission reaction of ^{241}Am.

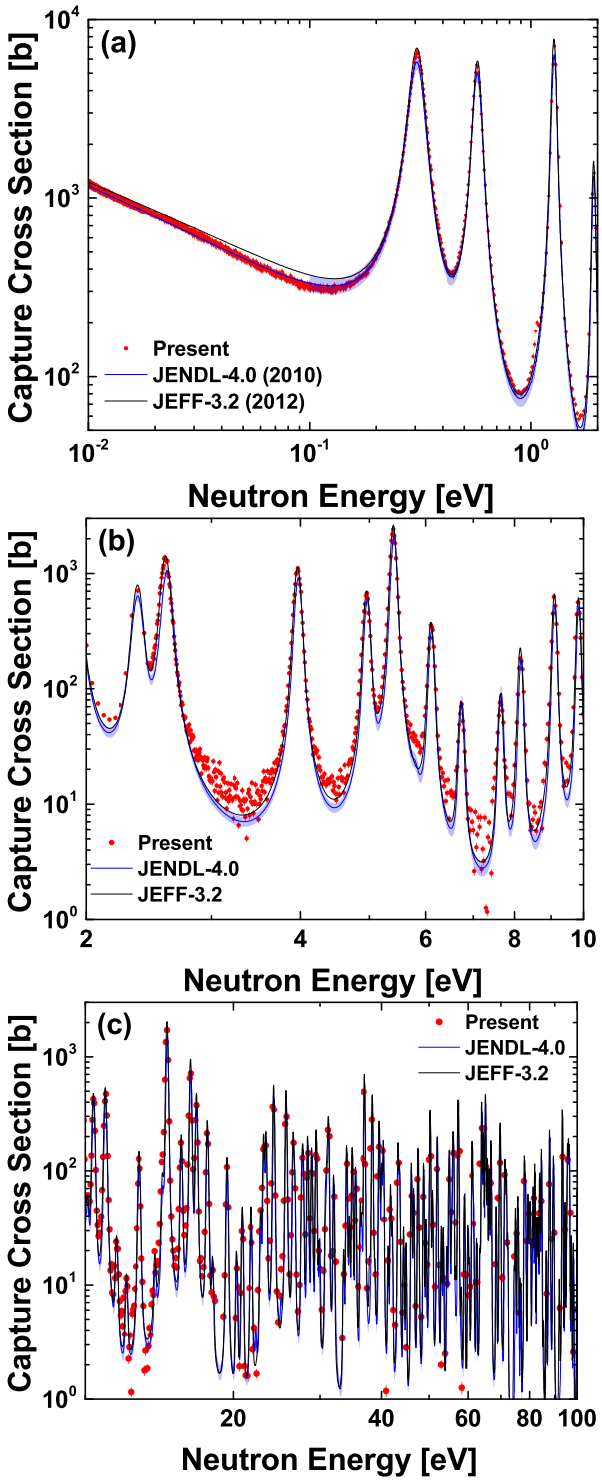

Figure 18 The determined neutron capture cross sections of ^{241}Am.

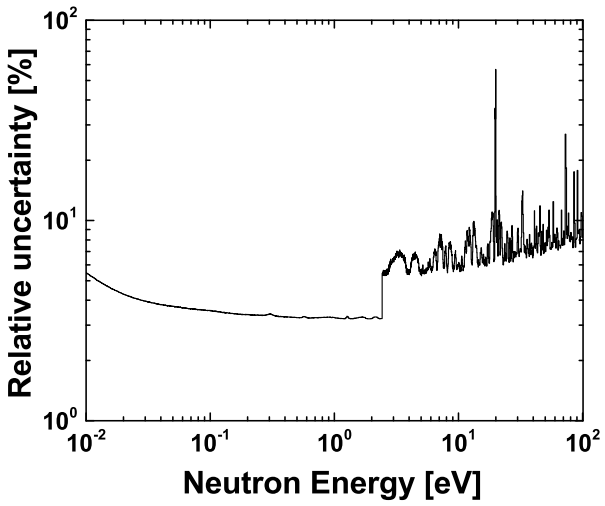

Figure 19 The uncertainties of the derived neutron capture cross sections of ^{241}Am. A step appeared at neutron energy of 2.4 eV following a change of the TOF bin width